Supporting Information

Three in One: Atomically dispersed Na boosting the photoreactivity of carbon nitride towards NO oxidation

Xiaofang Li, Zhao Hu, Qin Li, Ming Lei, Jiajie Fan, Sónia A.C. Carabineiro, Yi Liu*and Kangle Lv*

Synthesis

Typically, 10.0 g of dicyandiamide (DCDA) and 0.02 g of sodium bicarbonate ($NaHCO_3$) were dispersed into 160 mL of deionized water under magnetic stirring, and keep stirring for 30 min. Then the suspension was transferred into a 200 mL Teflon-lined autoclave and maintained at 160 ºC for 12 h. The solution was thoroughly evaporated at 80 ºC in an oven. The obtained white powders of amidinourea precursor were ground into a fine powder and calcined in a muffle furnace at 550 ºC for 2 h (10 ºC min^{-1}). The obtained yellow powders were filtered and washed with distilled water and dried in air under 60 ºC. The resulting sample was named as CN-Na2.

By varying the amount of $NaHCO_3$, we obtained a series of single atomic Na anchored CN samples (Table 1).

Evaluation of the photocatalytic activity

Photocatalytic oxidation of NO was carried out in a continuous-flow reactor (4.5 L) with a LED lamp ($\lambda > 420$ nm) as the light source that simulates sunlight (set-up see Fig. S1). Briefly, 0.02 g of the photocatalyst was dispersed into 30 mL of deionized water to form suspensions. After ultrasonication for 10 min, the suspensions were transferred into a culture dish (11 cm of diameter) and heated at 60 ^oC for 12 h for evaporation. The obtained photocatalyst film was put into the photochemical reactor. Before irradiation, NO and air were mixed in a bottle, while the concentration of NO was adjusted by a mass flow controllers. After reaching NO adsorption-desorption equilibrium (about 550 ppb), the photocatalytic reaction begins as soon as the LED lamp is turned on. The concentrations of NO and the accompanying NO_2 were detected online at the exit of the reactor by a

chemiluminescence NO_x analyzer (Advanced Pollution Instrumentation, Teledyne Technologies, USA).

To evaluate the reusablity of the Na-SA/CN-NSs photocatalyst, 5 succcessive runs for the photocatalytic oxidation of NO over CN-Na2 were carried out. After each run (irradiation for 30 min), 20 mL of water was added into the culture dish containing photocatalyst, which was then heated at 80 ^{o}C in an oven for 4 h to remove the surface adsorbed intermediates. After cooling down to room temperature, the dried dish was put into the reactor for the next photocatalytic reaction.

Characterization

The powder X-ray diffraction (XRD) patterns were carried out in a D8 X-ray diffractometer equipment (Cu-Kα radiation, λ= 0.15406 nm). The FTIR spectrum was obtained from the NEXUIS-470 infrared spectrometer equipment (Nicolet Co., U.S.A.). SEM was performed on a Hitachi S-4800 electron microscope. TEM were performed on Tecnai G20, USA. The HAADF-STEM characterization and energy-dispersive X-ray spectroscopy mapping images were performed on a Cs-corrected Titan Themis 60-300 (FEI, USA, 200 kV). X-ray photoelectron spectroscopy (XPS) data was performed on Multilab 2000 XPS system. UV-vis diffuse reflectance spectra (DRS) were collected on a dry-pressed disk samples with a UV-vis spectrophotometer (UV-2550, Shimadzu, Japan). Brunauer-Emmett-Teller (BET) specific surface areas and pore size distribution curve were performed on ASAP 2020 (Micromeritic Instruments, USA). Photoluminescence (PL) spectra were measured by a fluorescence spectrophotometer (F-7000, Hitachi, Japan) with an excitation wavelength of 350 nm. Time-resolved PL spectrum was collected on an Edinburgh FLS920 (Edinburgh Instruments Ltd, Edinburgh, England). Specimens for electron spin-resonance (ESR)

spectra was performed in DMPO solution under irradiation by an LED lample (λ > 400 nm). The DMPO-O_2^- and DMPO-•OH were carried out by dispersion in methanol and aqueous, respectively.

(Photo)electrochemical measurements

Transient photocurrent, Mott-Schottky plots and electrochemical impedance spectroscopy (EIS) Nyquist plots were performed on an electrochemical workstation (CHI760e, Shanghai, China). The detection was performed in a standard three-electrode system. Pt plate, ITO/CN electrode and Ag/AgCl electrode were used as counter electrode, working electrode and reference electrode, respectively. The ITO/CN electrode was produced by a drip coating method. A 3W LED lamp (λ = 420 ± 10 nm) purchased from Shenzhen LAMPLIC (China) was used as the light source, and Na_2SO_4 aqueous solution (0.4 $molL^{-1}$) was used as the electrolyte.

DFT calculations

All spin-polarized DFT-D2 calculations were conducted by the "Vienna Ab- initio Simulation Package" (VASP code 5.4.1) through the generalized gradient correlation function. The Cut-off energy and Gaussian trailing width were set to 400 eV and 0.2 eV, respectively. The Brillouin zone was adopted by a 3×3×1 Monkhorst Pack grid. All structures and energy were converged to below 0.01 eV. A 2×2×3 supercell of bulky CN was first relaxed.

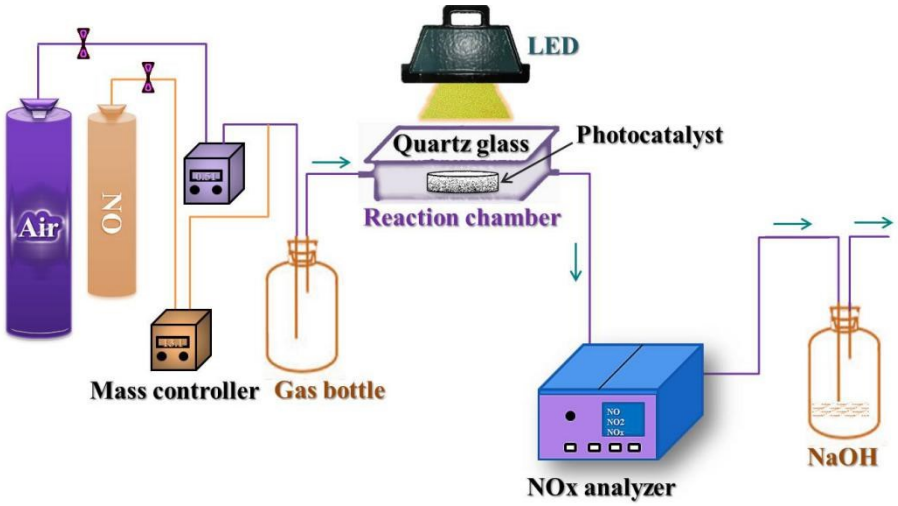

Fig. S1. Experimental set-up for the photocatalytic oxidation of NO in a continuous flow reactor[1].

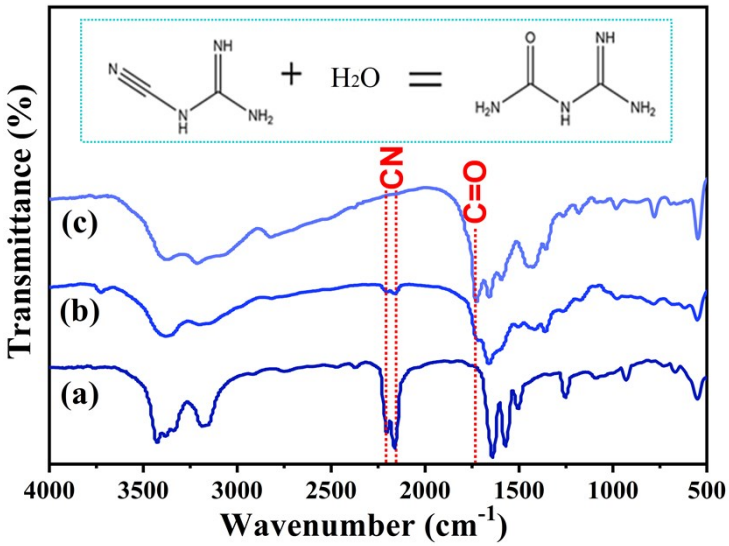

Fig. S2. FT-IR spectra of the precursors used for the synthesis of carbon nitride photocatalysts: DCDA (a), hydrolyzed DCDA (b) and hydrolyzed DCDA in $NaHCO_3$ solution (c).

To obtain a CN sample with a large BET surface area, we prepared CN nanosheets by polymerization of amidinourea, which can be obtained from the hydrolysis of DCDA. Fig. S1 shows the FTIR spectra of DCDA before and after hydrolysis. In Fig. S2a, we can clearly observe the strong absorption bands between 2260-2210 cm^{-1} from DCDA, typical of the infrared vibration of the cyano group (-CN). After hydrolyzation of DCDA in water, the IR absorption peaks for the –CN group dramatically decreased and, simultaneously, a new sharp peak at 1720 cm^{-1} appeared, which is characteristic of the vibration of the carbonyl group (C=O) (Fig. S2b). The decrease of the –CN groups and the production of C=O moieties during the hydrolysis of DCDA indicates the production of amidinourea (Eq. inset). In the presence of $NaHCO_3$, the reaction for the transformation of DCDA into amidinourea is greatly accelerated (Fig. S2c).

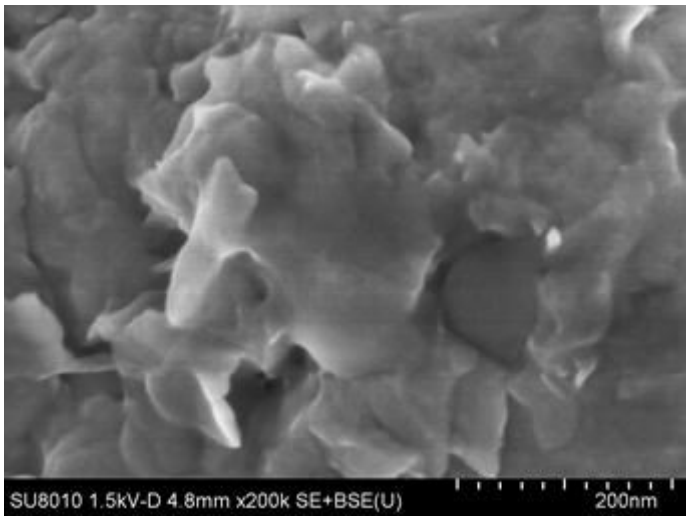

Fig. S3. SEM image of the CNB sample (bulky CN).

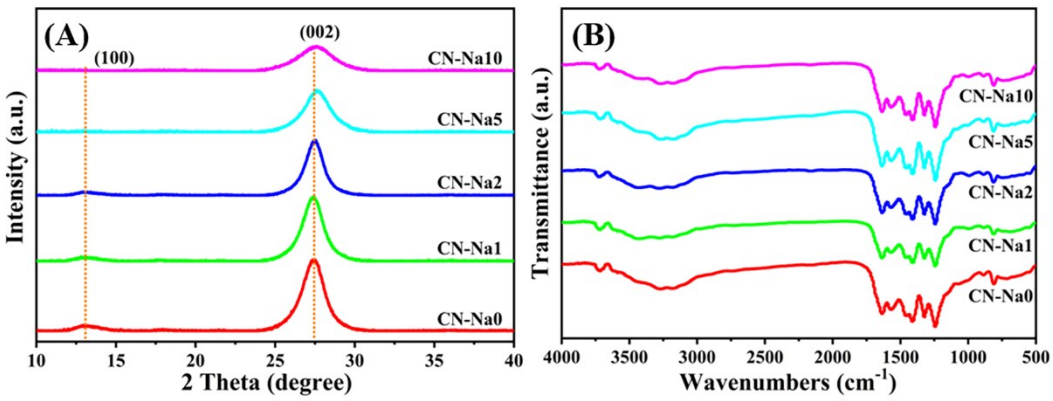

Fig. S4. XRD patterns (A) and FTIR spectra (B) of the CN-NSs samples.

Fig. S4A compares the XRD patterns of the CN nanosheet samples that were prepared in the presence of different amounts of $NaHCO_3$. It can be seen that all samples have two different diffraction peaks. The weak peak at 13º corresponds to the in-plane structural packing motifs of tri-s-triazine units, which is indexed as the (100) peak of CN, while the sharp peak centered at 27º is indexed as the (002) peak of CN, corresponding to interlayer stacking of aromatic segments. We can also see that the intensity of the two diffraction peaks decreases with the increase in the amount of $NaHCO_3$, indicating that the anchoring of Na retards the polymerization of CN nanosheets. The structure of CN is further confirmed by FTIR spectra, as shown in Fig. S4B, where the absorption peaks in the range of 1700-1200 cm^{-1} are attributed to the typical stretching modes of CN heterocycles, while the absorption at 810 cm^{-1} is characteristic of the triazine units of CN.

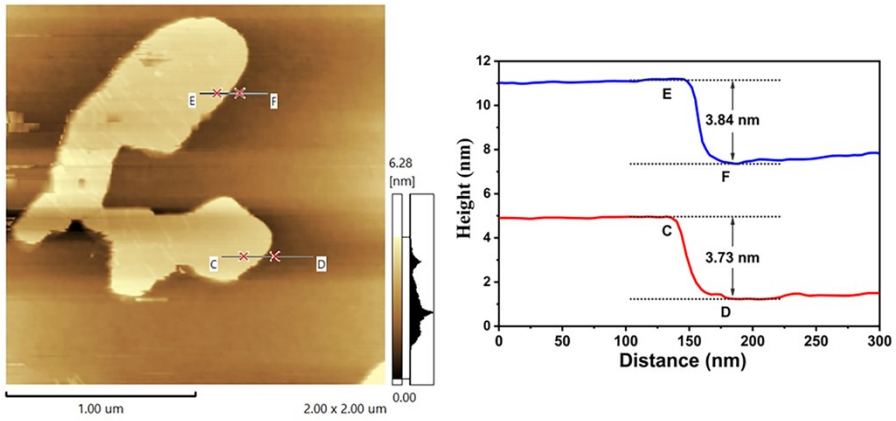

Fig. S5. AFM image of Na-SA/CN-NSs sample (CN-Na2).

The AFM image shown in of Fig. S5 shows that the thickness of Na-SA/CN-NSs (CN-Na2 sample) is about 3.7-3.8 nm, corresponding to the height of 10 molecular layers of CN.

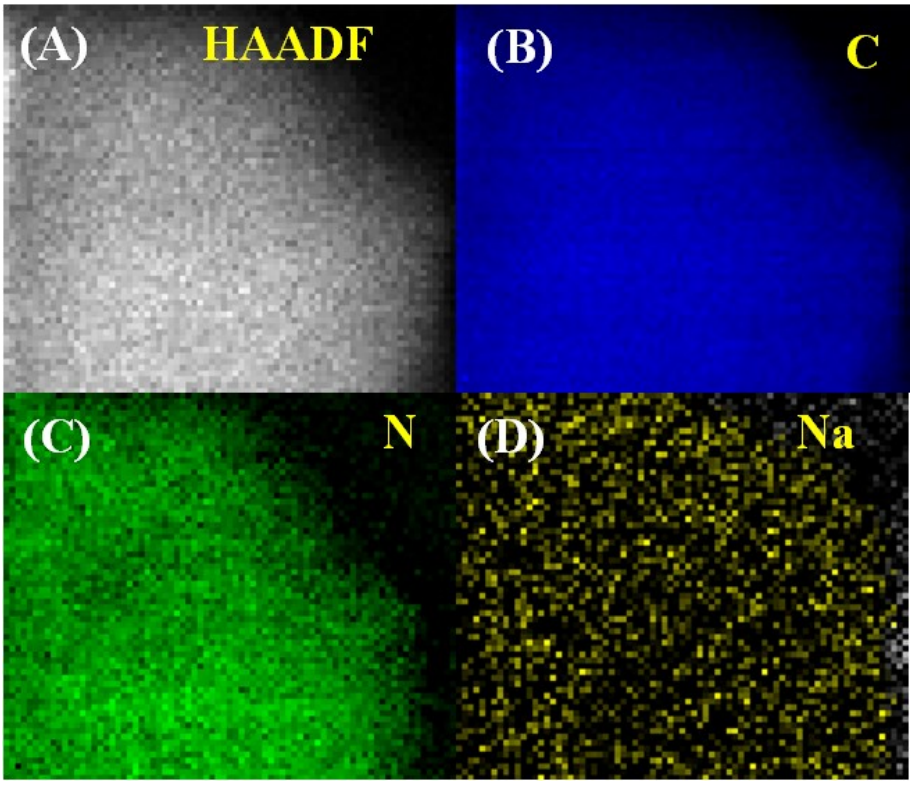

Fig. S6. STEM-DES elemental mapping of Na-SA/CN-NSs sample (CN-Na2).

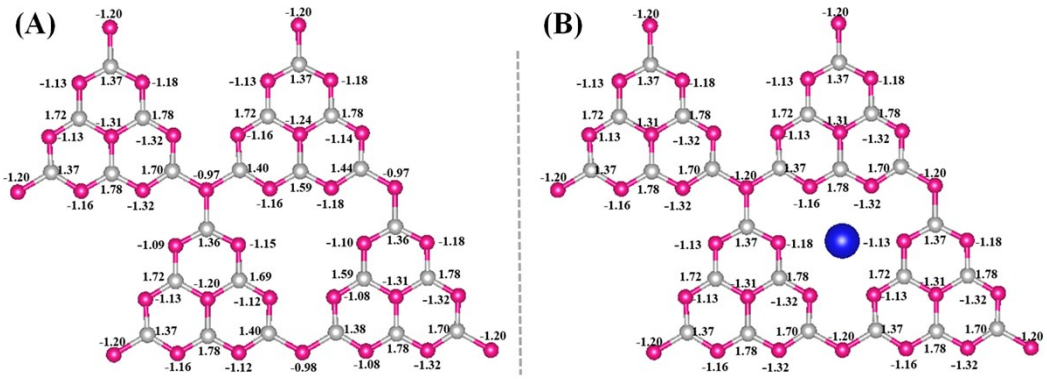

Fig. S7. Comparing the Bader effective charge of CN before and after anchorage of single atomic Na. Red, grey and blue spheres depict N, C and Na atoms, respectively.

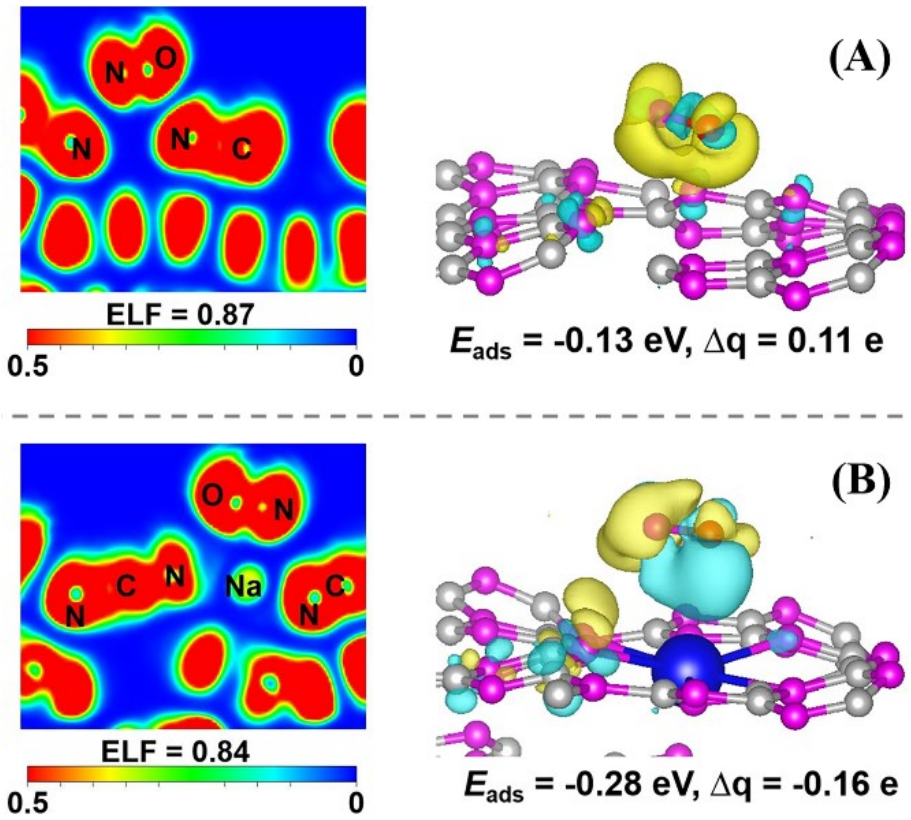

Fig. S8. Comparison of the electronic local function and the charge difference distribution of CN before (A) and after (B) anchorage of single atomic Na (charge accumulation and depletion in blue and yellow, respectively).

Fig. S8 shows that after anchoring CN with single atomic Na, the electronic local function of NO decreases from 0.87 to 0.84, and simultaneously the adsorption energy of NO over CN increases in magnitude from −0.13 eV to −0.28 eV, indicating that the length of the N-O bond is weakened due to the stronger chemical adsorption of NO on Na-SA/CN-NSs.

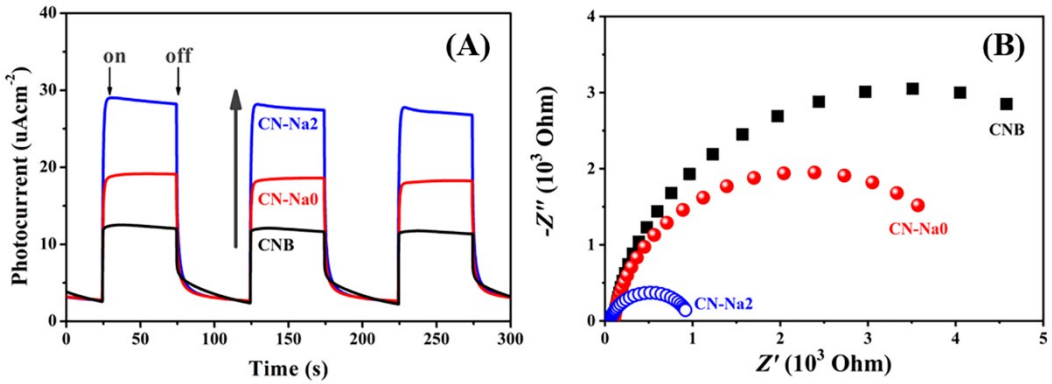

Fig. S9. Photocurrents (A) and electrochemical impedance spectroscopy (B) of the CN photocatalysts.

Fig. 9 shows that Na-SA/CN-NSs (CN-Na2 sample) possess the highest photocurrents, reflecting its accelerated charge transfer kinetics (Fig. S9A). The smallest arc radius on the EIS Nyquist plot of CN-Na2 sample (among all the other photocatalysts) also indicates its faster interfacial charge migration (Fig. S9B).

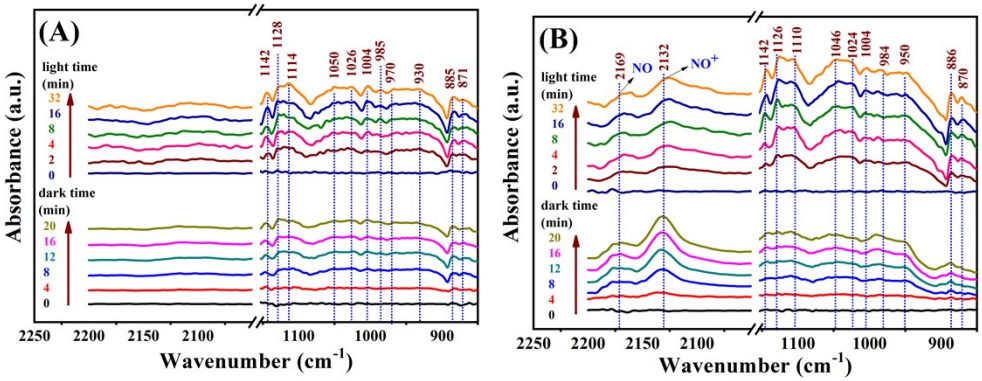

Fig. S10. *In-situ* DRIFTS recording the adsorption and photocatalytic oxidation of NO over CN-Na0 (A) and CN-Na2 samples (B).

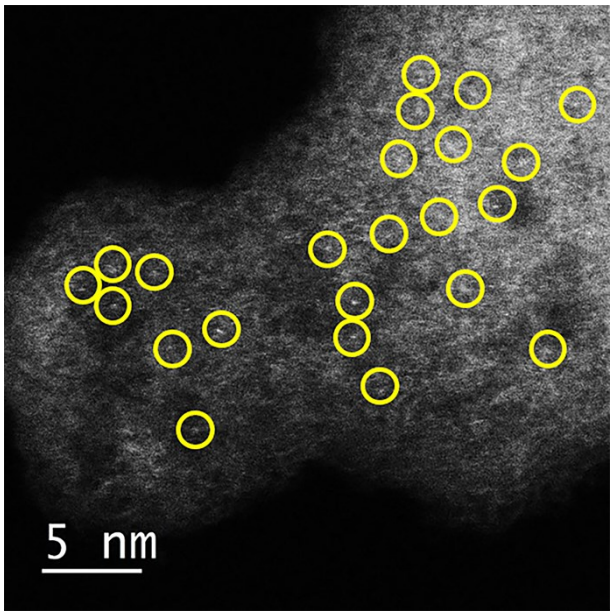

Fig. S11. HAADF-STEM image of atomically dispersed K anchored CN-NSs (single atom K sites in the HAADF-STEM image are highlighted by yellow circles).

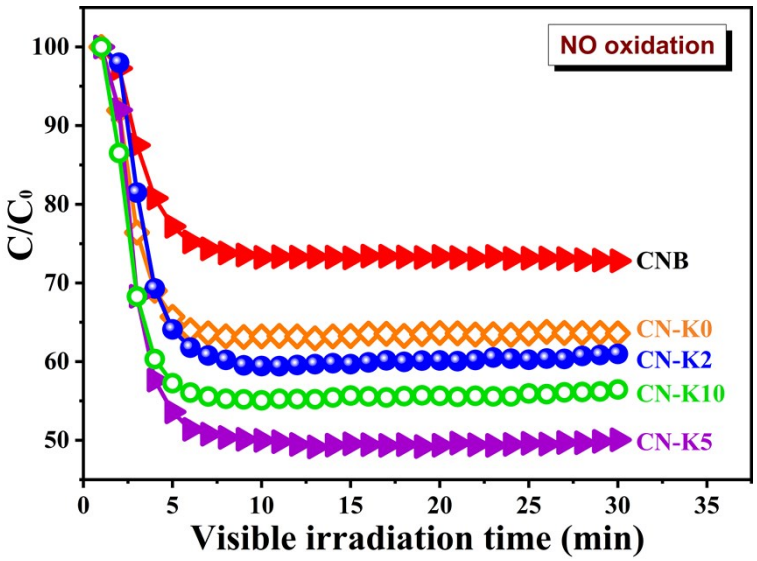

Fig. S12. Effect of K amount on the visible photocatalytic oxidation of NO over K-SA/CN-NS.

Table S1. Starting materials for C_3N_4 samples and their physical properties.

Samples[a]	Starting materials		Nitrogen sorption results[b]			Concentration	
	DCDA (g)	$NaHCO_3$ (g)	S_{BET} (m^2g^{-1})	APS (nm)	PV (cm^3g^{-1})	Na[c] (mgg^{-1})	NO_3^{-}[d] (mgg^{-1})
CN-Na0	10.0	0	28	16.5	0.12	--	0.85
CN-Na1	10.0	0.1	24	17.2	0.11	2.24	0.51
CN-Na2	10.0	0.2	24	21.2	0.13	3.72	0.91
CN-Na5	10.0	0.5	11	19.8	0.06	10.48	0.35
CN-Na10	10.0	1.0	5	19.4	0.02	17.51	0.54
CNB	10.0	0	7	25.1	0.04	--	0.35

[a]CNB represents bulky C_3N_4 sample which was prepared by directly calcination of DCDA powders without pre-hydrolysis.

[b]S_{BET}, APS and PV represent the BET surface area, average pore size and pore volume of the photocatalyst.

[c]Concentration of Na in the photocatalyst detected by inductively coupled plasma optic emission spectrometer (ICPOES 7030).

[d]Concentration of NO_3^- adsorbed on the surface of carbon nitride detected by ion chromatography (TOSOH IC-2010).

Table S2. Assignments of the DRIFTS bands observed during NO adsorption over Na-SA/CN-NSs.

Wavenumbers (cm^{-1})	Assignment	References	Wavenumbers (cm^{-1})	Assignment	References
2169	N_2O	[2]	1004	Bridging nitrates	[3]
2132	NO^+	[2a, 2c-e]	985, 984	Chelated nitrates	[2d, 4]
1142	NO^-/NOH	[3a, 3c, 4a]	970	Chelated nitrates	[2d, 4]
1128, 1126	NO^-	[5]	950	N_2O_3	[4a, 6]
1114, 1110	Monodentate nitrite/ Bidentate nitrates	[3b, 4a, 7]	930	N_2O_4	[6]
1050, 1046	Bidentate nitrates	[3a, 3b]	886,885	NO_2^-	[4a, 6]
1026, 1024	Monodentate nitrite	[4a, 7]	871, 870	Chelated nitrites	[2b, 4a]
1050, 1046	Bidentate nitrates	[3a, 3b, 4a]			

References

1 Z. Hu, K. N. Li, .X. F. Wu, N. Wang, X. F. Li, Q. Li, L. Li, K. L. Lv, *Appl. Catal. B: Environ.* **2019**, *256*, 117860.

2 a) J. Li, X. a. Dong, Y. Sun, G. Jiang, Y. Chu, S. C. Lee, F. Dong, *Appl. Catal. B: Environ.* **2018**, *239*, 187-195; b) K. I. Hadjiivanov, *Catal. Rev.* **2000**, *42*, 71-144; c) J. Li, M. Ran, P. Chen, W. Cui, J. Li, Y. Sun, G. Jiang, Y. Zhou, F. Dong, *Catal. Sci. Technol.* **2019**, *9*, 4531-4537; d) M. Kantcheva, *J. Catal.* **2001**, *204*, 479-494; e) T. Weingand, S. Kuba, K. Hadjiivanov, H. Knözinger, *J. Catal.* **2002**, *209*, 539-546.

3 a) J. Laane, J.R. Ohlsen, *Prog. Inorg. Chem.* **1980**, *27*, 465-513; b) J. Wu, Y. Cheng, *J. Catal.* **2006**, *237*, 393-404; c) W. Cui, J. Li, F. Dong, Y. Sun, G. Jiang, W. Cen, S. C. Lee, Z. Wu, *Environ. Sci. Technol.* **2017**, *51*, 10682-10690.

4 a) Y. Li, M. Gu, M. Zhang, X. Zhang, K. Lv, Y. Liu, W. Ho, F. Dong, *Chem. Eng. J.* **2020**, *389*, 124421; b) Y. Zhou, Z. Zhao, F. Wang, K. Cao, D. E. Doronkin, F. Dong, J. D. Grunwaldt, *J. Hazard. Mater.* **2016**, *307*, 163-172.

5 a) T. Xiong, H. Wang, Y. Zhou, Y. Sun, W. Cen, H. Huang, Y. Zhang, F. Dong, *Nanoscale* **2018**, *10*, 8066-8074; b) N. Tang, Y. Liu, H. Wang, Z. Wu, *J. Phys. Chem. C* **2011**, *115*, 8214-8220.

6 V. A. Konstantin Hadjiivanov, Dimitar Klissurski, T. Marinova, *Langmuir* **2002**, *18*, 1619-1625.

7 M. Kantcheva, *J. Catal.* **2004**, *223*, 352-363.